Magnetic relaxation and dissipative heating in ferrofluids

P. P. Vaishnava, R. Tackett, A. Dixit, C. Sudakar, R. Naik, and G. Lawes

Citation: Journal of Applied Physics **102**, 063914 (2007); doi: 10.1063/1.2784080
View online: http://dx.doi.org/10.1063/1.2784080
View Table of Contents: http://scitation.aip.org/content/aip/journal/jap/102/6?ver=pdfcov
Published by the AIP Publishing

Magnetic relaxation and dissipative heating in ferrofluids

P. P. Vaishnava
Department of Physics, Kettering University, Flint, Michigan 48504, USA

R. Tackett, A. Dixit, C. Sudakar, R. Naik, and G. Lawes[a)]
Department of Physics and Astronomy, Wayne State University, Detroit, Michigan 48201, USA

(Received 29 June 2007; accepted 2 August 2007; published online 28 September 2007)

We have investigated the ac magnetic susceptibility and magnetic heating of aqueous suspensions of γ-Fe_2O_3 nanoparticles embedded in alginate hydrogel matrix and isolated γ-Fe_2O_3 and Fe_3O_4 nanoparticles coated with tetramethyl ammonium hydroxide. All three ferrofluids were characterized by measuring the dc magnetization, ac susceptibility, and magnetic heating. We found that significant Néel relaxation is present in all samples, but only the isolated nanoparticle ferrofluids show any significant feature associated with Brownian relaxation near the freezing temperature of the carrier liquid. The heating rate of the ferrofluids varies systematically with the magnitude of the Brownian relaxation peak, despite similar values of the absolute magnetization. These results highlight the importance of the Brownian relaxation for heating applications incorporating magnetic nanoparticles. © *2007 American Institute of Physics*.
[DOI: 10.1063/1.2784080]

INTRODUCTION

Colloidal suspensions of nanometer size magnetic particles in a carrier liquid, called a *ferrofluid*, have been proposed for a range of biomedical applications, which are summarized in Refs. 1 and 2, and references therein. Some of these applications include magnetic separation,[3,4] targeted drug delivery,[5,6] and contrast enhancement of magnetic resonance imaging.[7–9] The response of magnetic nanoparticles to a time varying magnetic field has led to the suggestion that ferrofluids could be used for hyperthermia, a treatment delivering a toxic amount of thermal energy to neoplastic cells in the body.[10] Hyperthermia has been shown to be a potentially effective therapeutic modality in cancer treatment as it intensifies the efficacy of radiation and chemotherapy.[11] Most biomedical applications require a large magnetic moment per formula unit, making iron oxides such as Fe_3O_4 (bulk saturation magnetic moment of M_s=75 emu/g at room temperatures) and γ-Fe_2O_3 (M_s=82 emu/g) attractive choices for these uses.[12]

The two mechanisms most responsible for magnetic relaxation in nanoparticles, and subsequently most of the heat dissipated by nanoparticles in ferrofluids, are the physical rotation of the individual particles in the fluid (Brownian relaxation) and the collective rotation of the atomic magnetic moments within each particle (Néel relaxation).[13,14] For Néel relaxation, the energy barrier for magnetization reorientation is determined by the magnetocrystalline anisotropy, while for Brownian relaxation, it is determined by viscosity and particle size.[15] Both of these relaxation mechanisms are single particle effects; interparticle interactions can affect magnetic dynamics in highly concentrated samples.[16] The principles underlining the heating of magnetic nanoparticles in a ferrofluid, reviewed by Rosensweig,[13] are based on the Debye model. For small field amplitudes (H), the power (P) dissipated by the changing magnetization in a ferrofluid in an ac field (frequency f) is given by

$$P = \mu_0 \pi f \chi'' H^2, \tag{1}$$

where χ'' is the frequency dependent out-of-phase susceptibility. Typical values of the magnetic field used for hyperthermia applications are between 1 and 15 kA/m, at frequencies from 50 to 500 kHz.[17,18] Equation (1) predicts a linear relation between the dissipated power and the out-of-phase susceptibility of the ferrofluid.

The hydrodynamic properties of ferrofluids have been extensively studied.[19–22] However, most of the experimental studies on the role of Brownian and Néel mechanisms for determining the power dissipated as magnetic heating in ferrofluids have relied on immobilizing nanoparticle rotation (suppressing Brownian relaxation) by adding epoxy or similar material to irreversibly solidify the sample.[23,24] Because it is impossible to verify that the solidification does not affect the distribution of nanoparticles, it is preferable to suppress the Brownian relaxation reversibly. In order to accomplish this goal, we have investigated the temperature dependence of the magnetic properties of ferrofluids to probe the effect of Brownian relaxation. While the magnetic heating measurements are always done in the liquid phase, where both Brownian and Néel relaxations may be relevant, we can study the relative importance of these two mechanisms by investigating the magnetic response at the crossover between the low temperature solid (no Brownian relaxation) and the high temperature liquid (Brownian relaxation possible) phases.

SAMPLE PREPARATION

Alginate hydrogels are polysaccharides composed of α-L-guluronic acid and mannuronic acid residues arranged in homopolymorphic and alternating blocks. We prepared

[a)]Author to whom correspondence should be addressed. Electronic mail: glawes@wayne.edu

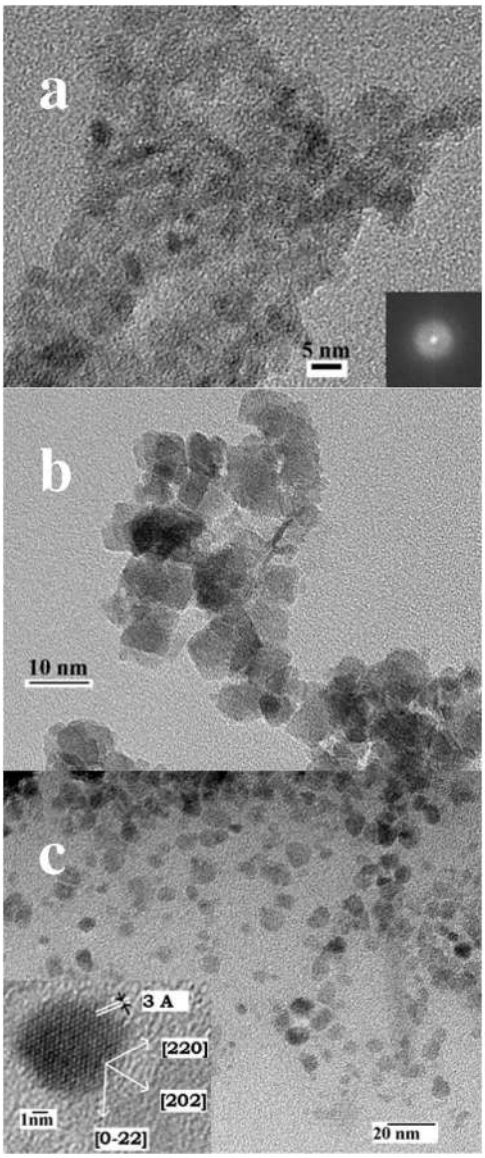

FIG. 1. TEM images of (a) γ-Fe_2O_3 nanoparticles embedded in a larger alginate nanoparticle (AGFO), (b) γ-Fe_2O_3 nanoparticles with a TMAH surfactant (TGFO), and (c) Fe_3O_4 nanoparticles with a TMAH surfactant (TFO). The inset of panel (a) shows a FFT of the AGFO sample, while the inset of panel (c) shows a high-resolution image of a single Fe_3O_4 nanoparticle with the crystal planes labeled. Note that the scale bars are different for all three panels.

γ-Fe_2O_3 nanoparticles in alginate hydrogel (sample AGFO) using the method outlined in Ref. 25. This method produces small γ-Fe_2O_3 magnetic crystallites embedded inside a larger alginate nanoparticles, as can be seen in the transmission electron microscope (TEM) image in Fig. 1(a) (discussed in the next section). The average hydrodynamic diameter of the alginate nanoparticle was determined to be approximately 50 nm using dynamic light scattering (DLS), confirmed by fluorescence correlation spectroscopy. The Fe_3O_4 ferrofluid (sample TFO) sample was prepared by coprecipitation, with 4 ml of 1*M* $FeCl_3$ aqueous solution mixed in a beaker with 1 ml of 2*M* solution of $FeCl_2$ aqueous solution. We then added 50 ml of 1*M* ammonium hydroxide solution. The black precipitate of magnetite was rinsed several times with de-ionized water before 1 ml of 25% tetramethyl ammonium hydroxide (TMAH) was added to the solution to prevent agglomeration of the magnetic nanoparticles. A third γ-Fe_2O_3 ferrofluid (sample TGFO) sample was prepared by oxidizing Fe_3O_4 obtained above by using 5% H_2O_2 solution and heating to 60 °C. TMAH is added to stabilize these particles in the solution. We have focused on understanding very dilute ferrofluids for two reasons. First, investigating dilute solutions will allow us to neglect the role of interactions, both magnetic and steric. Second, dilute samples may be a more appropriate model for many biomedical applications. However, because we are measuring dilute samples, the heating rates are significantly smaller than what has been observed in hyperthermia measurements on more concentrated samples.[24,26]

RESULTS AND DISCUSSION

All three samples were characterized by x-ray diffraction (XRD) and TEM. The XRD spectra (not shown) showed that the samples were crystalline and had the expected crystal structures. We determined the size distribution for each sample by measuring the diameters of many nanoparticles from the TEM images shown in Fig. 1 and fitting the resulting histogram with a Gaussian distribution. The average diameter of the γ-Fe_2O_3 nanoparticles embedded in alginate (AGFO) was determined to be 6 nm and the average diameters for the TMAH coated γ-Fe_2O_3 and Fe_3O_4 ferrofluid samples were determined to be 8 and 6 nm, respectively. All three nanoparticle samples were relatively polydisperse, with a standard deviation in the diameter of approximately 2 nm for all samples. While one expects a slight increase in nanoparticle size when converting Fe_3O_4 to γ-Fe_2O_3, we attribute this volume change mainly to some particle growth by accretion due to the elevated temperature during oxidation.

Figure 1(a) shows the γ-Fe_2O_3 nanoparticles (small darker spots) clustered inside the much larger alginate nanoparticle (lighter spot). The inset plots a fast Fourier transform (FFT) of this image, which shows mainly the diffuse scattering from the alginate nanoparticle. The images are consistent with several magnetic nanoparticles being embedded in the same alginate nanoparticle, and the size of the lighter spot representing the alginate nanoparticle is consistent with the DLS measurements. Conversely, the TEM images of the TGFO and TFO samples [Figs. 1(b) and 1(c), respectively] show considerably more isolated nanoparticles, with no evidence for structural connections between individual nanoparticles. The inset of Fig. 1(c) shows a high-resolution TEM image of a single Fe_3O_4 nanoparticle, in which the atomic planes are clearly visible, emphasizing the crystalline structure of these nanoparticles.

We measured the dc magnetization of the ferrofluid samples between 2 and 330 K using a Quantum Design magnetic property measurement system (MPMS) superconducting quantum interference device (SQUID) magnetometer. Because the measurements are done in vacuum, we sealed the liquid samples inside Stycast 1266 epoxy cylinders. We measured the ac susceptibility of these samples between 2 and 330 K at frequencies between 0.02 and 10 kHz using the AC susceptibility and DC magnetization (ACMS) option on

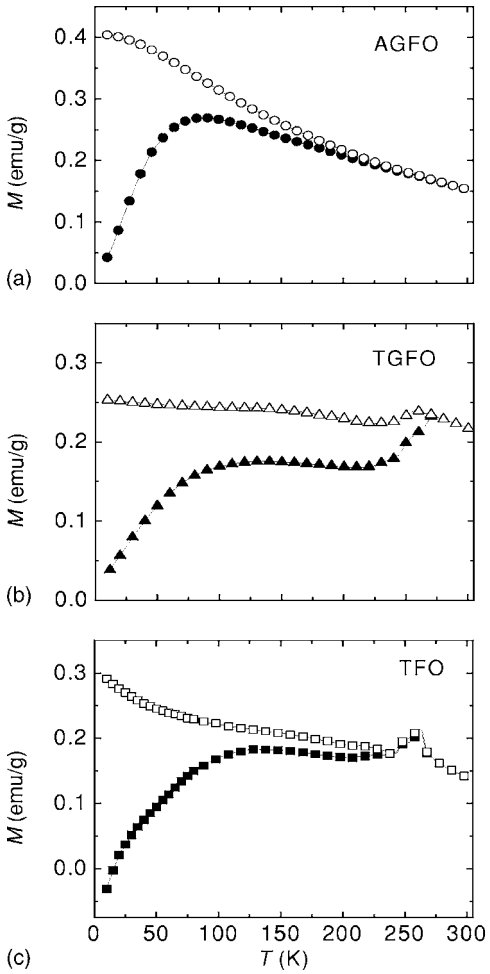

FIG. 2. The magnetization vs temperature for both zero field cooled (filled symbols) and field cooled (open symbols) magnetizations measured with a dc field of 100 Oe is shown in (a) for AGFO (γ-Fe_2O_3 in alginate matrix), (b) for TGFO (γ-Fe_2O_3 coated with TMAH), and (c) for TFO (Fe_3O_4 coated with TMAH).

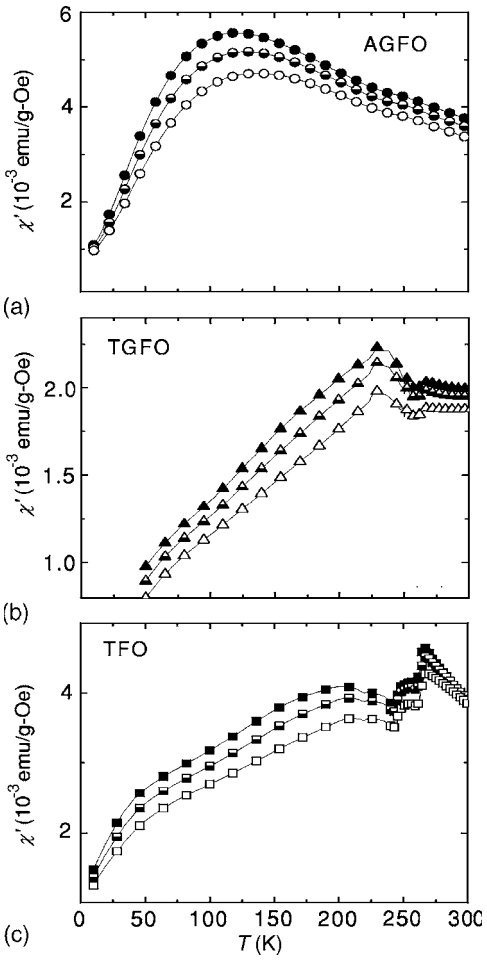

FIG. 3. The temperature dependence of the real susceptibility (χ') at frequencies of 100 Hz (open symbols), 1 kHz (half-filled symbols), and 10 kHz (closed symbols) for (a) AGFO (γ-Fe_2O_3 in alginate), (b) TGFO (γ-Fe_2O_3 coated with TMAH), and (c) TFO (Fe_3O_4 coated with TMAH).

a Quantum Design physical property measurement system (PPMS). For the hyperthermia measurements, 5 ml of each sample was placed in a plastic vial and held inside a 2 cm long solenoid with a total of 27 turns. An ac field with strength of 250 Oe was produced by using a Hefler amplifier operating at 125 kHz. The samples were thermally isolated from the solenoid using a high density Styrofoam cladding. The temperature change of the sample due to resistive heating in the coil was negligible, which we verified using deionized water as a control.

The magnetization versus temperature for the AGFO sample for both zero field cooled (ZFC) and FC magnetizations is shown in Fig. 2(a). For all panels in Fig. 2, data collected under ZFC conditions are represented by solid symbols, while data collected under field cooling are represented with open symbols. The blocking temperature T_B for AGFO sample is approximately 85 K. Similar peaks in the ZFC curve [Figs. 2(b) and 2(c)] are observed for the Fe_3O_4 ferrofluid (TFO) and γ-Fe_2O_3 (TGFO) samples, where the blocking temperatures are 125 and 118 K, respectively. We also note that there is a large magnetic anomaly associated with the freezing of the carrier fluid for the TFO and TGFO samples at approximately 270 K, but no such freezing signature is present in the AGFO sample. We will discuss this feature in more detail in the following. We can estimate the magnetocrystalline anisotropy from the blocking temperature using the relation $KV=25k_BT_B$, appropriate for dc magnetic measurements.[27] Using this expression, we find that for the AGFO sample $K=3\times10^6$ ergs/cc, for the TFO sample $K=3\times10^6$ ergs/cc, and for the TGFO sample $K=1\times10^6$ ergs/cc. All the K values are significantly greater than the values for the bulk γ-Fe_2O_3 ($K=4.7\times10^4$ ergs/cc) and Fe_3O_4 ($K=6.4\times10^4$ ergs/cc).[28] Our K values are close to the 1.35×10^6 ergs/cc for Fe_3O_4 suspended in water obtained by Ma *et al.*[29] and $(1.02-1.4)\times10^6$ ergs/cc for maghemite particles hosted in silica aerogel pores by Fernandez *et al.*[30]

We have investigated the magnetic dynamics of the three ferrofluids to further study the energy dissipation mechanisms present in the samples. Figure 3 shows the temperature dependence of the real (χ') susceptibility for frequencies between 100 Hz and 10 kHz. For the AGFO sample [Fig. 3(a)], χ' shows a broad maximum around 125 K, which can be associated with superparamagnetic blocking. The other two samples, TGFO and TFO in Figs. 3(b) and 3(c), respectively, rather show an ac susceptibility that increases monotonically with temperature until almost 300 K, consistent with the

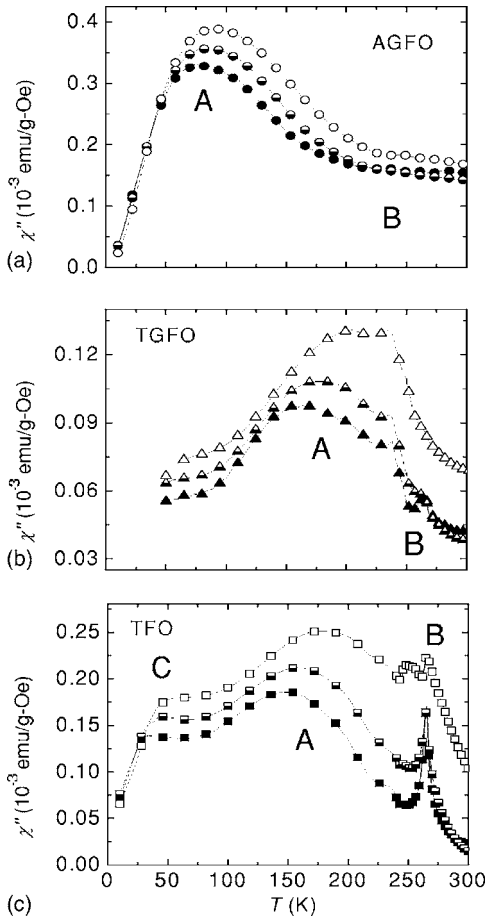

FIG. 4. The temperature dependence of the imaginary part (χ'') of susceptibility for frequencies of 100 Hz (open symbols), 1 kHz (half-filled symbols), and 10 kHz (closed symbols) for (a) AGFO (the γ-Fe_2O_3 in alginate), (b) TGFO (γ-Fe_2O_3 coated with TMAH), and (c) TFO (Fe_3O_4 coated with TMAH).

larger blocking temperature of these samples. Additionally, both TMAH samples show a sharp anomaly at the freezing temperature of the carrier fluid, which we associate with the onset of Brownian relaxation as the suspension melts.

The relaxational dynamics of the samples can be seen more easily by looking at the ac magnetic dissipation. Figure 4 plots the imaginary part, $\chi''(T)$, of the susceptibility for the three ferrofluids between 100 Hz and 10 kHz. The AGFO sample [Fig. 4(a)] shows two distinct peaks. The larger peak (labeled A), occurring at approximately 100 K, shifts to a higher temperature with increasing frequency. Because the carrier fluid is frozen at low temperatures, the nanoparticles are fixed at 100 K, so peak A must correspond to Néel relaxation of the magnetic moment. This observed frequency dependence is consistent with thermally activated Néel relaxation. There is a second, almost unnoticeable peak (labeled B), which has no discernable frequency dependence. We associate peak B with the onset of Brownian relaxation in the ferrofluid at the melting temperature of the carrier liquid, although the small size of this anomaly suggests that the Brownian relaxation is negligible in the AGFO sample. We argue that the Brownian relaxation is never significant in the alginate samples because several magnetic iron oxide nanoparticles are embedded in the much larger alginate particles

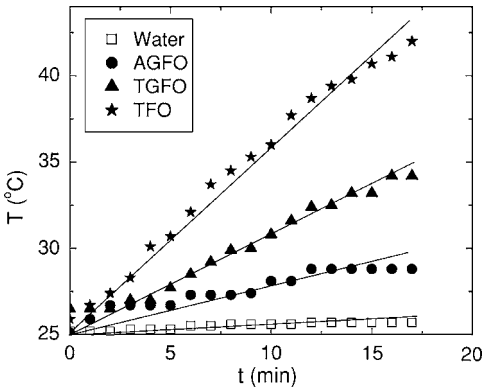

FIG. 5. The temperature vs time plots for the AGFO (γ-Fe_2O_3 in alginate), TGFO (γ-Fe_2O_3 coated with TMAH), and TFO (Fe_3O_4 coated with TMAH) samples heated by a 250 Oe ac magnetic field at 125 kHz. The heating curve for a pure water (DIUF) sample is also included as a reference. The solid lines drawn through data are intended as guides to the eye.

(~50 nm). Because of this configuration, single nanoparticle rotation is strongly suppressed, so Brownian motion does not play a significant role in magnetic relaxation for this sample.

For TGFO and TFO samples the out-of-phase component shows two distinct peaks at 170 and 267 K [Figs. 4(b) and 4(c)]. Peak A at approximately 170 K corresponds to Néel relaxation, and peak B at ~270 K arises from Brownian relaxation associated with the melting of the carrier liquid. In the frozen state, the solid carrier solution completely suppresses any Brownian motion of the nanoparticles. However, close to the melting transition, the effective viscosity of the carrier liquid is very large,[31] leading to a peak in magnetic dissipation due to Brownian relaxation. The TFO sample shows a third anomaly, denoted as peak C. This peak has some small frequency dependence, and we tentatively attributed this feature to relaxation processes involving the surface spins. Contributions from surface spins are thought to be responsible for the reduced magnetization in small nanoparticles,[32–34] and are believed to undergo a spin-glass transition well below the nanoparticle blocking temperature.[35]

In order to determine the magnetic power loss in these ferrofluids, we performed heating experiments in ac magnetic fields on all three samples. Figure 5 shows the temperature versus time for the samples in the presence of ac magnetic field with amplitude of 250 Oe at a frequency of 125 kHz. The heating curve for a pure water [de-ionized ultrafiltered (DIUF)] sample is also included as a control. The solid line through each set of data is intended as a guide to the eye. We find that there is only negligible heating in the (nonmagnetic) water, suggesting that the increase in temperature in the ferrofluid samples is driven almost entirely by magnetic relaxation effects. The slope ($\Delta T/\Delta t$) is smallest for the γ-Fe_2O_3 in alginate samples, higher for the γ-Fe_2O_3 in TMAH samples, and highest for the Fe_3O_4 in TMAH ferrofluid. This slope is related to the power dissipated due to magnetic relaxation, assuming that the specific heat is approximately the same for all ferrofluid samples, which is reasonable given the very dilute nature of the samples. It should be noted that the volume susceptibilities for all three samples are similar, so the differences in heating rate cannot

be attributed to much higher concentrations of magnetic material in one particular sample. In fact, the sample with the smallest heating (AGFO) has the largest magnetization. In separate studies, we have found that the heating rate in ferrofluids can be increased substantially by raising the concentration of magnetic nanoparticles, as predicted by Eq. (1).[36]

We can qualitatively understand the differences in heating by examining the mechanisms for energy dissipation at the freezing temperature for the three samples. The AGFO sample shows only a negligible peak in $\chi''(T)$ at the freezing temperature. This suggests that there is never any significant Brownian relaxation present in this system. This is consistent with the observation that multiple small γ-Fe_2O_3 nanoparticles are randomly embedded in a single larger alginate nanoparticle. Conversely, TMAH surfacted Fe_3O_4 nanoparticles (TFO) and γ-Fe_2O_3 nanoparticles (TGFO) show much larger anomalies in χ'' at freezing, consistent with more significant Brownian relaxation. The AGFO sample, with no significant Brownian relaxation, shows only small heating. The TGFO sample, with moderate Brownian relaxation, shows intermediate heating, while the TFO sample, with the largest Brownian relaxation (determined by the magnitude of the peak in χ'' at freezing) shows the largest heating. Our investigations support the suggestion that the Brownian relaxation is the dominant mechanism for heat production in magnetic nanoparticle suspensions, even for particles smaller than 10 nm, contrary to some suggestions.[37]

In summary, we have studied the dc magnetization, ac susceptibility, and hyperthermia characteristics of γ-Fe_2O_3 nanoparticles (average size of ~6 nm) embedded in alginate hydrogel matrix and Fe_3O_4 nanoparticles (average size of ~6 nm) and γ-Fe_2O_3 nanoparticles (average size of ~8 nm) coated with tetramethyl ammonium hydroxide. All ferrofluids show a clear Néel relaxation, but by studying the magnetic dissipation near the freezing temperature, we find that the Brownian relaxation is only significant for the isolated nanoparticle samples, TFO and TGFO, while the nanoparticles in alginate, AGFO, show a minimal Brownian relaxation. This suggests that the Brownian relaxation is likely the dominant source for energy dissipation for isolated nanoparticle.

ACKNOWLEDGMENTS

We would like to acknowledge the Richard J. Barber Funds for Interdisciplinary Research, the Institute for Manufacturing Research at Wayne State University, and the donors of the American Chemical Society (PRF No. 46160-G10) for supporting this research. We thank Paul Keyes and Nick Powell for providing the dynamical light scattering data and Ashis Mukhopadhyah for fluorescent correlation spectroscopy measurements on the alginate nanoparticle sample.

[1]D. Leslie-Pelecky, V. Labhasetwar, and R. H. Krauss, Jr., in *Advanced Magnetic Nanostructures*, edited by D. J. Sellmyer and R. Skomski (Springer, New York, 2006).
[2]Q. A. Pankhurst, J. Connolly, S. K. Jones, and J. Dobson, J. Phys. D **36**, R167 (2003).
[3]R. S. Molday and D. Mackenzie, J. Immunol. Methods **52**, 353 (1982).
[4]N. Seesod, P. Nopparat, A. Hedrum, A. Holder, S. Thaithong, S. Uhlen, and J. Lindberg, Am. J. Trop. Med. Hyg. **56**, 322 (1997).
[5]H. Pardoe, W. Chua-Anusorn, T. G. St. Pierre, and J. Dobson, J. Magn. Magn. Mater. **225**, 41 (2001).
[6]J. L. Arias, V. Gallordo, S. Gomez-Lopera, R. C. Plaza, and A. V. Delgado, Cytokines Cell Mol. Ther. **77**, 309 (2001).
[7]R. Lawaczeck, H. Bauer, T. Frenzel, M. Hasegawa, Y. Ito, K. Kito, N. Miwa, H. Tsutsui, H. Volger, and H. J. Weinmann, Acta Radiol. **38**, 584 (1997).
[8]R. Weissleder, G. Elizondo, J. Wittenberg, C. A. Rabito, H. H. Bengele, and L. Josephson, Radiology **175**, 489 (1990).
[9]R. Weissleder, A. Moore, U. Mahmood, R. Bhorade, H. Benveniste, E. A. Chiocca, and J. P. Bassilion, Nat. Med. **6**, 351 (2000).
[10]A. Jordan, P. Wust, H. Fahling, W. John, A. Hinz, and R. Felix, Int. J. Hyperthermia **9**, 51 (1993).
[11]O. S. Nielson, M. Horsman, and J. Overgaard, Eur. J. Cancer **37**, 1587 (2001).
[12]L. F. Gamarra, G. E. S. Brito, W. M. Pontuschka, E. Amaro, A. H. C. Parma, and G. F. Goya, J. Magn. Magn. Mater. **289**, 439 (2005).
[13]R. E. Rosensweig, J. Magn. Magn. Mater. **252**, 370 (2002).
[14]R. Hergt, W. Andra, C. G. d'Ambly, I. W. Kaiser, U. Richter, and H.-G. Shmidt, IEEE Trans. Magn. **34**, 3745 (1998).
[15]J. Frenkel, *The Kinetic Theory of Liquids* (Dover, New York, 1955).
[16]R. W. Chantrell, M. El-Hilo, and K. O'Grady, IEEE Trans. Magn. **27**, 3570 (1991).
[17]I. Hilger, W. Andra, R. Hergt, R. Hiegeist, H. Schubert, and W. A. Kaiser, Radiology **18**, 570 (2001).
[18]D. C. F. Chan, D. B. Kirpotin, and P. A. Bunn, J. Magn. Magn. Mater. **122**, 374 (1993).
[19]T. Jonsson, P. Svedlindth, and M. F. Hansen, Phys. Rev. Lett. **81**, 3976 (1998).
[20]S. H. Chung, A. Hoffmann, S. D. Bader, C. Liu, B. Kay, L. Makowski, and L. Chen, Appl. Phys. Lett. **85**, 2971 (2004).
[21]Y. Bao, A. B. Pakhomov, and K. M. Krishnan, J. Appl. Phys. **99**, 08H107 (2006).
[22]B. H. Erne, K. Butter, B. W. M. Kuipers, and G. J. Vroege, Langmuir **19**, 8218 (2003).
[23]K. Okawa, M. Sekine, M. Maeda, M. Tada, M. Abe, N. Matsushita, K. Nishio, and H. Handa, J. Appl. Phys. **99**, 08H102 (2006).
[24]I. Baker, Q. Zeng, W. Li, and C. R. Sullivan, J. Appl. Phys. **99**, 08H106 (2006).
[25]R. Naik, U. Senaratne, N. Powell, E. C. Buc, G. M. Tsoi, V. M. Naik, P. P. Vaishnava, and L. E. Wenger, J. Appl. Phys. **97**, 10J313 (2005).
[26]J. Giri, P. Pradhan, T. Sriharsha, and D. Bahadur, J. Appl. Phys. **97**, 10Q916 (2005).
[27]C. de Julian Fernandez, Phys. Rev. B **72**, 054438 (2005).
[28]G. Bates, *Magnetic Oxides*, edited by D. J. Craik (Wiley, London, 1975), p. 689.
[29]M. Ma, Y. Wu, J. Zhou, Y. Sun, Y. Zhang, and N. Gu, J. Magn. Magn. Mater. **268**, 33 (2004).
[30]M. B. Fernandez van Raap, F. H. Sanchez, C. E. Rodriguez Torres, L. I. Casas, A. Roig, and E. Molins, J. Phys.: Condens. Matter **17**, 6519 (2005).
[31]S. Bae, S. W. Lee, and Y. Takemura, Appl. Phys. Lett. **89**, 252503 (2006).
[32]J. M. D. Coey, Phys. Rev. Lett. **27**, 1140 (1971).
[33]P. P. Vaishnava, U. Senaratne, E. C. Buc, R. Naik, V. M. Naik, G. M. Tsoi, and L. E. Wenger, Phys. Rev. B **76**, 024413 (2007).
[34]T. Sato, T. Iijima, M. Seki, and N. Inagaki, J. Magn. Magn. Mater. **65**, 252 (1987).
[35]B. Martinez, X. Obradors, L. Balcells, A. Rouanet, and C. Monty, Phys. Rev. Lett. **80**, 181 (1998).
[36]A. Dixit, R. Tackett, C. Sudakar, P. P. Vaishnava, R. Naik, and G. Lawes (unpublished).
[37]J. Connolly and T. G. St. Pierre, J. Magn. Magn. Mater. **225**, 156 (2001).